

Identification of nm23-H1 as a metastatic suppressor and prognostic factor in nasopharyngeal carcinoma by proteomic analysis

LI Xuebing¹, HU Rong², QU Jiaquan², HE Qiuyan², CHEN Yu², LI Jiaoyang², YE Xu², XIANG Yali², YI Hong²

(1.Department of Gerontology, Xiangya Hospital, Central South University, Changsha 410008; 2.Key Laboratory of Cancer Proteomics of Chinese Ministry of Health, Xiangya Hospital, Central South University, Changsha 410008, China)

ABSTRACT

Objective: To identify proteins associated with nasopharyngeal carcinoma (NPC) metastasis, and provide scientific basis for the prevention and cure of NPC.

Methods: A two-dimensional gel electrophoresis and mass spectrometry were performed to screen for differential proteins between highly metastatic 5-8F and non-metastatic 6-10B NPC cell lines. Western blot was used to confirm the differential proteins. We siRNA used to inhibit the expression of differential protein nm23-H1 to determine the association of nm23-H1 with NPC in vitro invasive ability. Immunohistochemistry and statistics were used to evaluate the correlation of nm23-H1 expression with clinicopathological features and clinical outcomes in paraffin-embedded archival tissues including 93 cases of primary NPC and 20 cases of cervical lymphonode metastatic NPC (LMNPC).

Results: A total of 15 differential proteins in the 2 cell lines were identified by a proteomic approach, and 3 differential proteins were selectively confirmed. Downregulation of nm23-H1 by siRNA significantly increased the in vitro invasive ability of 6-10B. Significant nm23-H1 downregulation was observed in LMNPC compared with primary NPC. nm23-H1 downregulation in primary NPC was positively correlated with lymphonode and distant metastasis, advanced clinical stage and recurrence. Survival curves showed that patients with nm23-H1 downregulation in primary NPC had a poor prognosis. Multivariate analysis confirmed that nm23-H1 expression level in primary NPC was an independent prognostic indicator.

Conclusion: nm23-H1 behaves as a metastasis suppressor in NPC, and nm23-H1 downregulation in the is a biomarker for poor NPC prognosis.

KEY WORDS

nasopharyngeal carcinoma; proteomics; nm23-H1; metastasis; prognosis

DOI:10.3969/j.issn.1672-7347.2012.01.004

蛋白质组学方法识别 nm23-H1 为鼻咽癌的转移抑制蛋白和预后因子

李雪兵¹, 胡蓉², 瞿家权², 贺秋艳², 陈瑜², 李娇阳², 叶旭², 向亚莉², 易红²

(中南大学湘雅医院 1. 老干科, 长沙 410008; 2. 卫生部肿瘤蛋白质组学重点实验室, 长沙 410008)

Date of reception: 2011-10-07

Biography: LI Xuebing, senior Nurse, mainly engaged in the research of cancer proteomics.

Corresponding author: YI Hong, Email: yh1126@hotmail.com

Foundation items: This work was supported by National Nature Science Foundation of China (30973290, 81172559, 81172302), Key Research Program from Science and Technology Department of Hunan Province, China (2010FJ2009), and Nature Science Foundation of Hunan Province, China (11JJ2045).

[摘要] 目的: 筛选鼻咽癌(NPC)转移相关蛋白质,为鼻咽癌防治提供科学依据。**方法:** 采用二维电泳和质谱技术筛选不同转移潜能鼻咽癌细胞系(5-8F和6-10B)的差异表达蛋白质,并应用Western印迹对部分差异蛋白质进行验证;使用siRNA抑制差异蛋白质nm23-H1的表达,分析nm23-H1表达水平对鼻咽癌细胞体外侵袭能力的影响;应用免疫组织化学染色分析nm23-H1表达水平与鼻咽癌临床病理特征和预后的关系。**结果:** 在不同转移潜能鼻咽癌细胞系中鉴定了15个差异表达的蛋白质,并选择性证实3个差异蛋白质;siRNA下调nm23-H1的表达能增强6-10B鼻咽癌细胞的体外侵袭能力;淋巴结转移鼻咽癌组织中nm23-H1的水平显著低于原发性鼻咽癌;nm23-H1的表达水平与鼻咽癌淋巴结和远处转移、临床分期和复发正相关;生存分析显示nm23-H1低表达的鼻咽癌患者预后差;多因素分析显示:nm23-H1表达水平是鼻咽癌患者独立的预后因子。**结论:** nm23-H1是鼻咽癌的转移抑制蛋白和预后因子。

[关键词] 鼻咽癌;蛋白质组学;nm23-H1;转移;预后

Nasopharyngeal carcinoma (NPC) is one of the most common malignant tumors in southern China and Southeast Asia^[1]. NPC is notorious for its potential to metastasize at the early stages of the disease^[2-4]. For the NPC patients who have a distant metastasis, the outcome was generally ominous, with >98% of the patients eventually dying of disease^[5-6]. But the molecular mechanism underlying metastasis of NPC remains unclear. Identification of NPC metastasis-associated factors is helpful not only for understanding the mechanisms involved in NPC metastasis, but also for finding biomarkers for prognosis and potential therapeutic targets of NPC.

High throughput technologies such as microarrays and proteomics offer the potential ability to find alterations previously unidentified in NPC. Analyses for gene expression profiles of NPC have been reported using a cDNA array, found the genes with aberrant expressions possibly contributed to metastasis of NPC^[7-8]. Proteomics has introduced a new approach to cancer research which aims at identifying differential expression proteins associated with the development and progression of cancer, providing new opportunities to uncover biomarkers and therapeutic targets for cancer as well as reveal the molecular mechanism underlying this disease^[9]. A major obstacle, however, to proteomic analysis of tumor specimens is tissue heterogeneity, which is particularly relevant to NPC as it often includes numerous infiltrating lymphocytes and stroma. Using cancer cell lines may be an alternative way to find biomarkers and therapeutic targets for cancer by proteomics.

The NPC cell lines 5-8F and 6-10B with different metastatic potentials are ideal for investigation of the quantitative and qualitative changes involved in tumor metastasis. Both cell sublines originated from the SUNE-1 NPC cell line and have the same genetic background^[10-11]. Previous work by Song et al^[12] has shown that the metastatic ability of the two cell sublines in nude mice clearly differed: 5-8F had highly metastatic ability and distant metastasis occurred after 4 weeks (8/8, 100%)

while 6-10B had no metastatic ability at all (0/8).

In this study, we used a proteomic approach to compare the protein expression profiles of 5-8F and 6-10B cell lines to identify proteins related to NPC metastasis. The results showed that the expression level of nm23-H1, one of the differential proteins, was significantly lower in highly metastatic 5-8F than in non-metastatic 6-10B. Because the accumulating evidence indicated that nm23-H1 was involved in the metastasis of human malignant tumors, and its expression level was associated with the patient prognosis, we tested whether nm23-H1 could inhibit the metastasis of NPC, and also evaluated clinicopathological significances of nm23-H1 in NPC.

I Materials and methods

1.1 Materials

1.1.1 Reagents

Immobiline pH-gradient (IPG) DryStrips (pH3-10, length 24 cm), IPG buffer (pH3-10), and the second antibodies-conjugated with horseradish peroxidase were purchased from Amersham Biosciences (USA). Rabbit polyclonal antibody against nm23-H1 was from Santa Cruz Biotechnology (USA). Rabbit polyclonal antibody against annexin A1 was from Abcam Inc.(USA). Mouse monoclonal antibody against CK8 was from Lab Vision Corp.(USA).

1.1.2 Cell lines and tissue specimens

5-8F and 6-10B NPC cell lines were kindly provided by the Cancer Center, Sun Yat-sen University, China^[14]. Formalin-fixed and paraffin-embedded archival tissue specimens including 93 cases of primary NPC and 20 cases of cervical lymphonode metastatic NPC (LMNPC) between 1996 and 2000 were obtained from the Cancer Hospital of Hunan Province, China, according to institutional regulation. Based on the 1978 WHO classification, all primary tumors and LMNPC were histopathologically diagnosed as poorly differentiated or undifferentiated carcinoma. The clinical stage of all the patients was classified or reclassified according to the 1992 NPC staging system of China^[13]. All the patients received radical radiotherapy and were given follow-up. The

follow-up period at the time of analysis was 6 to 72 (48±14.5) months.

1.2 Methods

1.2.1 Two-dimensional gel electrophoresis

5-8F and 6-10B cells were lysed in lysis buffer (7 mol/L urea, 2 mol/L thiourea, 100 mmol/L DTT, 4% CHAPS, 40 mmol/L Tris, 2% Pharmalyte, 1 mg/mL DNase I) at 37 °C for 1 h, followed by centrifugation at 15000 r/min for 30 min at 4°C. The concentration of the total proteins was determined using 2D quantification kit (Amersham Biosciences). Two-dimensional gel electrophoresis (2-DE) was performed to separate 600 g protein samples as previously described by us^[14]. After 2-DE, the blue silver staining was used to visualize the protein spots in the 2-DE gels.

1.2.2 Image analysis

The stained 2-DE gels were scanned with MagicScan software on an Imagescanner (Amersham Biosciences, USA), and analyzed by using a PDQuest system (Bio-Rad Laboratories, USA) according to the protocols provided by the manufacturer. To minimize the contribution of experimental variations, 3 separate gels were prepared for each cell line. The gel spot pattern of each gel was summarized in a standard after spot matching. Thus, we obtained one standard gel for each cell line. These standards were then matched to yield information about protein spots related to the NPC metastasis. The following criteria for differential protein expression were used: spot intensity ≥ 2 -fold increased or decreased in 5-8F in comparison to 6-10B (Significant differences in protein expression levels were determined by Student's *t*-test with a set value of $P < 0.05$).

1.2.3 Protein identification by MS

All the differential protein spots were excised from stained gels using punch, and in-gel trypsin digestion was performed as previously described by us^[14]. The tryptic peptide was analyzed with a Voyager System DE-STR 4307 MALDI-TOF MS (ABI) to get a peptide mass fingerprint (PMF). In PMF map database searching, peptide matching and protein searches against the Swiss-Prot database were performed using the Mascot search engine (<http://www.matrixscience.com/>) with a mass tolerance of ± 50 part per million. The protein spots identified by MALDI-TOF-MS were also subjected to analysis of ESI-Q-TOF MS (Micromass; Waters). MS/MS spectra were performed in data-dependent mode in which up to 4 precursor ions above an intensity threshold of 7 counts/second (cps) were selected for MS/MS analysis from each survey "scan". In tandem mass spectrometry data database query, the peptide sequence tag (PKL) format file that generated from MS/MS was imported into the Mascot search engine

with a MS/MS tolerance of ± 0.3 Da to search the Swiss-Prot database.

1.2.4 Western blot

Forty microgram of lysates from 5-8F and 6-10B cells were separated by 10% SDS-PAGE, and transferred to a PVDF membrane. Blots were blocked with 5% nonfat dry milk for 2 h at room temperature (RT), and then incubated with primary antibody for 2 h at RT, followed by incubation with a horseradish peroxidase-conjugated secondary antibody for 1 h at RT. The signal was visualized with ECL detection reagent and quantitated by densitometry using ImageQuant image analysis system (Storm Optical Scanner, Molecular Dynamics). The mouse anti- β -actin antibody (Sigma-Aldrich) was detected simultaneously as a loading control.

1.2.5 Administration of nm23-H1 siRNA to 6-10B cells

The cells were transfected with nm23-H1 siRNA or control siRNA (Santa Cruz Biotechnology) according to the siRNA transfection protocol provided by the manufacturer. Briefly, the day before the transfection, 6-10B cells were plated into 6-well plates at the density of 10^5 cells/mL in RPMI 1640 medium (Invitrogen, USA) containing 10% FBS (Invitrogen, USA). When the cells were 60%-80% confluent, they were transfected with 10 nmol/L of nm23-H1 siRNA or control siRNA after a preincubation for 20 min with siRNA transfection reagent in siRNA transfection medium (Santa Cruz Biotechnology). Four hours after the beginning of the transfection, the medium was replaced with in RPMI 1640 medium containing 10% FBS, and continued to culture the cells for additional 44 h. At the end of the transfection, nm23-H1 expression level in the cells was determined by Western blot as described above.

1.2.6 In vitro cell invasion assay

The invasiveness of 6-10B cells transfected with nm23-H1 siRNA or control siRNA was evaluated in 24-well transwell chambers (Costar) as directed by the manufacturer. Briefly, the upper and lower culture compartments of each well were separated by polycarbonate membranes (8 μ m pore size). The membranes were pre-coated with 100 μ g/cm² of Matrigel (Collaborative Biomedical Products), which was reconstituted by adding 0.5 mL of serum-free RPMI 1640 medium to the well for 2 h. To assess the ability of the cells to penetrate the pre-coated polycarbonate membrane, 1.25×10^4 cells in 0.5 mL of RPMI 1640 medium containing 1% FBS were placed into the upper compartment of wells, and 0.75 mL of RPMI 1640 medium containing 10% FBS was placed into the lower compartment. The transwell chambers were incubated for 24 h at 37°C in humidified 5% CO₂ atmosphere. Invaded cells attached underneath the chamber membrane was stained with a Diff-Quik stain

kit (Dade Behring) and counted in 5 random fields with an inverted microscope. Invasive ability was defined as the average cell numbers that penetrated the matrix-coated membrane per field. Three independent experiments were performed in triplicate.

1.2.7 Immunohistochemistry and evaluation of staining

Immunohistochemical staining of nm23-H1 protein was performed on formalin-fixed and paraffin-embedded tissue sections using the standard immunohistochemical technique. Four-micrometer tissue sections were deparaffinized in xylene, rehydrated in a graded ethanol series, and treated with an antigen retrieval solution (10 mmol/L sodium citrate buffer, pH 6.0). The sections were incubated with a dilution of 1 : 100 rabbit polyclonal anti-human nm23-H1 antibody overnight at 4 C, and then were incubated with 1 : 1000 dilution of biotinylated secondary antibody followed by avidin-biotin peroxidase complex (DAKO) according to the manufacturer's instructions. Finally, tissue sections were incubated with 3', 3'-diaminobenzidine (Sigma-Aldrich) until a brown color developed, and counterstained with Harris' modified hematoxylin. In negative controls, primary antibodies were omitted.

nm23-H1 protein staining was assessed according to the methods previously described by us^[15]. Each case was rated according to a score that added a scale of intensity of staining to the area of staining. The intensity of staining was graded on the following scale: 0, no staining; 1+, mild staining; 2+, moderate staining; 3+, intense staining. The area of staining was evaluated as follows: 0, no staining of cells in any microscopic fields; 1+, <30% of tissue stained positive; 2+, between 30% and 60% stained positive; 3+, >60% stained positive. The minimum score when summed (extension + intensity) was therefore 0 and the maximum, 6. A combined staining score (extension + intensity) of ≤ 2 was considered to be negative; a score between 3 and 4 was considered to be moderate expression; that between 5 and 6 was considered to be high expression.

1.3 Statistical analysis

Statistical analysis was done by using SPSS (version 13.0). The significant difference of nm23-H1 protein expression between primary and metastatic tumors was determined by using the t-test. Significant differences between the nm23-H1 protein expression and clinical variables were compared by the Mann-Whitney U test or ANOVA test. Survival rates (cumulative survival, cumulative survival curves) were obtained by the Kaplan-Meier method, and the differences (between the curves) were compared by log-rank tests. The deaths caused by NPC were considered as outcomes; the deaths by other causes were censored and the missing values were replaced

by the series mean method. A univariate analysis with Cox proportional hazards model was used to determine each identified prognostic factor; multivariate analysis with the Cox proportional hazards model was used to explore combined effects. A difference of $P < 0.05$ was considered statistically significant. All P -values were two-tailed.

2 Results

2.1 Detection of differential proteins in 5-8F and 6-10B cell lines by 2-DE

To identify the proteins associated with the NPC metastasis, we initiated a comparative proteomic study of 5-8F and 6-10B NPC cell lines. Two representative 2-DE maps from 5-8F and 6-10B were shown in Figure 1A. A total of 21 protein spots that had consistent differences (≥ 2 -fold) between the 2 cell lines in triplicate experiments were chosen as differential protein spots and subjected to MS analysis, and 15 differential protein spots that had been identified by MS were marked with arrows in Figure 1A. Close-up of the region of the gels showing all 15 identified differential protein spots in 5-8F and 6-10B was shown in Figure 1B.

2.2 Identification of differential proteins by MS

All of 21 differential protein spots were analyzed by MALDI-TOF-MS and ESI-Q-TOF-MS. A total of 15 differential proteins were identified. The MALDI-TOF MS map and database query result of a representative spot 1 were shown in Figures 2A and 2B, respectively. A total of 35 monoisotopic peaks were input into Mascot search engine to search the Swiss-Prot database, and the query result showed that protein spot 1 was nm23-H1. The MS/MS results of spot 1 were shown in Figures 2C and 2D. The amino acid sequence of a triply charged peptide from spot 1 with m/z 706.0528 was identified as YMHSGPVVAMVWEGLNVVK, which was a part of nm23-H1 sequence, and the query result indicated that protein spot 1 was nm23-H1. The annotation of all the identified proteins was summarized in the Table 1.

2.3 Validation of the identified proteins

To confirm the expression levels of the differential proteins identified by a proteomic approach, the expression of three identified proteins (nm23-H1, keratin 8, and annexin A1) in 6-10B and 5-8F cell lines were detected by Western blot. As shown in Figures 3A and 3B, the expression of nm23-H1 and keratin 8 was significantly higher, whereas annexin A1 was significantly lower in 6-10B than 5-8F ($P < 0.01$), which confirms the results of proteomic analysis.

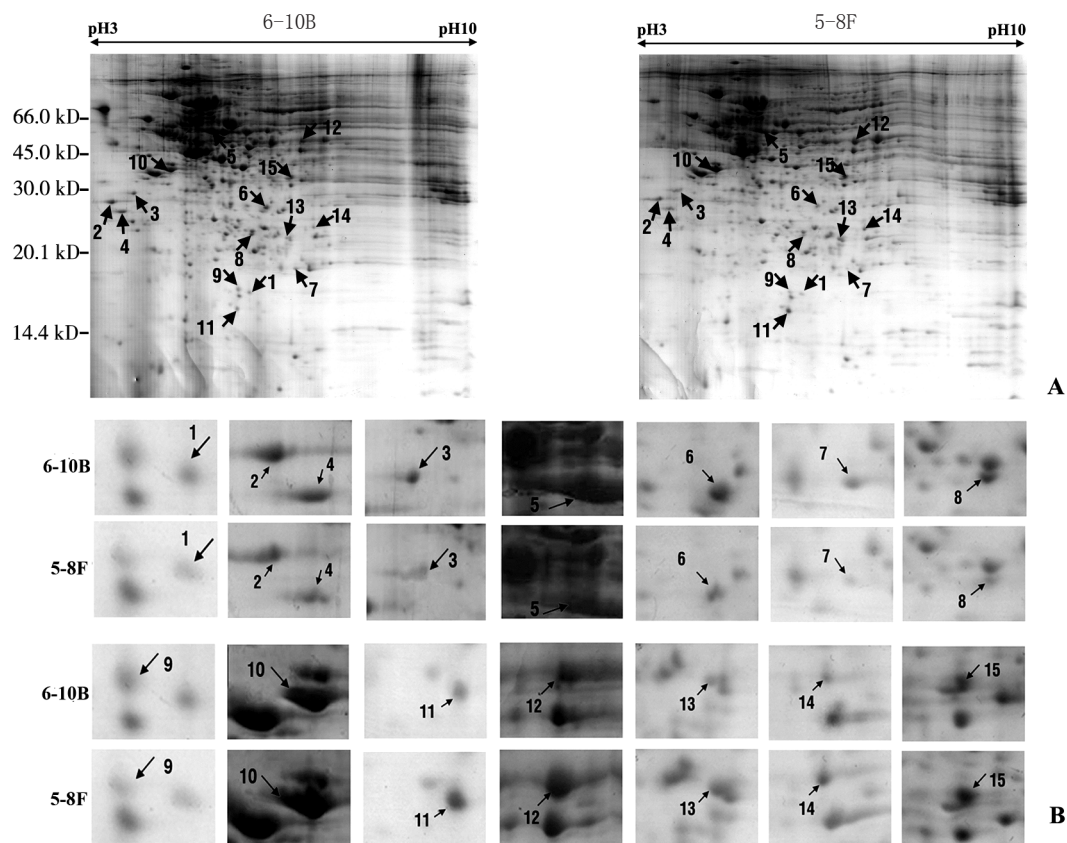


Figure 1 Representative 2-DE maps of 6-10B and 5-8F cell lines. Fifteen differential protein spots marked with arrows were identified using both MALDI-TOF-MS and ESI-Q-TOF-MS (A), and close-up image of all 15 identified differential protein spots in 5-8F and 6-10B cells(B).

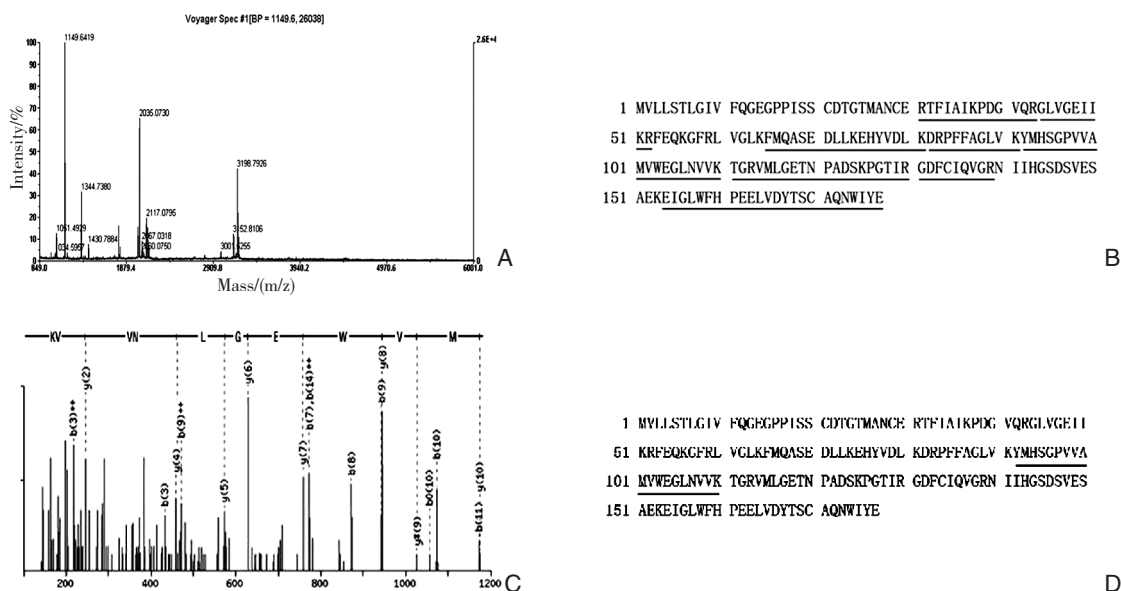


Figure 2 MALDI-TOF-MS and ESI-Q-TOF-MS analysis of differential protein spot 1. A: MALDI-TOF-MS mass spectrum of spot 1 identified as the nm23-H1 according to the matched peaks is shown; B: Protein sequence of nm23-H1 is shown, and matched peptides are underlined; C: ESI-Q-TOF-MS sequenced spectrum of spot 1. The amino acid sequence of a triply charged peptide with m/z 706.0528 is identified as YMHSGPVVAMVWEGLNVVK from mass differences in the y -fragment ions series, and matched with residues 92-110 of nm23-H1; D: Protein sequence of nm23-H1 is shown. Matched MS/MS fragmentation is underlined.

Table 1 Differential expression proteins between 6-10B and 5-8F identified by MALDI-TOF-MS and ESI-Q-TOF-MS

Spot No	Swiss-Prot AC	Protein name	MW (kD)	pI	Coverage	Fold change (6-10B/5-8F)
1	P15531	nm23-H1	19.87	5.42	67%	2.8
2	Q07021	subcomponent-binding protein	23.84	4.32	46%	2.1
3	P06753	tropomyosin alpha-3 chain	29.11	4.75	56%	4.0
4	P31947	14-3-3 protein sigma	27.87	4.68	73%	2.6
5	P05787	keratin 8	53.67	5.52	32%	4.4
6	Q13011	delta3, 5-delta2, 4-dienoyl-CoA isomerase	36.14	8.16	41%	3.0
7	Q96CJ1	ELL-associated factor 2	14.25	4.28	60%	8.9
8	P04792	HSP27	22.83	5.98	60%	2.2
9	P60174	triosephosphate isomerase	26.81	6.51	69%	2.1
10	P07910	hnRNP C1/C2	32.39	4.94	33%	0.48
11	Q45FD6	MHC class I antigen	21.12	5.43	34%	0.26
12	P06733	alpha-enolase	47.35	7.01	54%	0.36
13	P33316	deoxyuridine 5'-triphosphate nucleotidohydrolase	26.98	9.65	44%	0.37
14	P18669	phosphoglycerate mutase 1	28.77	6.75	45%	0.40
15	P04083	Annexin A1	38.79	6.57	57%	0.47

AC: accession code; Mw: molecular weight; pI: isoelectric point

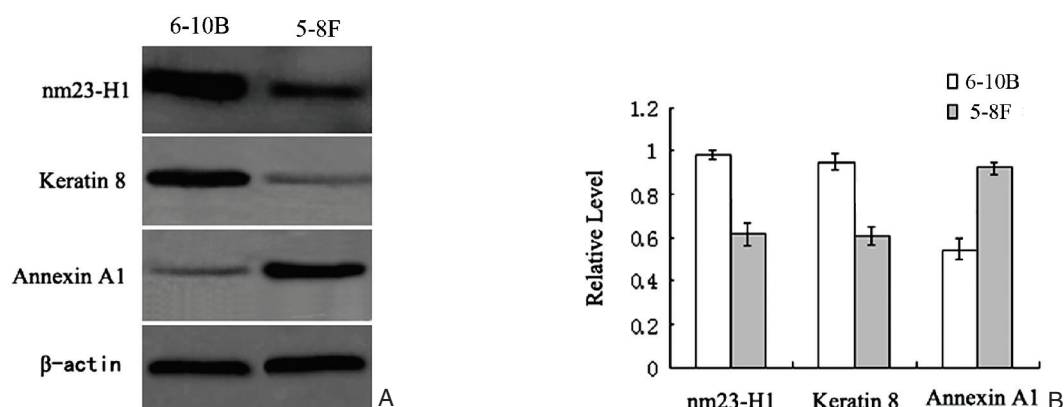


Figure 3 A representative result of Western blot of nm23-H1, keratin 8 and Annexin A1 in NPC cell lines 6-10B and 5-8F. β -actin was used as an internal control for loading. A: Western blot showing changes in expression levels of nm23-H1, keratin 8 and Annexin A1 in 5-8F and 6-10B cells; B: Histogram shows the expression levels of the three proteins in the 2 NPC cell lines as determined by densitometric analysis.

2.4 Effects of nm23-H1 knockdown by siRNA on cell invasion of 6-10B cells

To study the association of nm23-H1 expressional levels with its metastatic ability, 6-10B cells were transfected with nm23-H1 siRNA, and nm23-H1 expression was determined by Western blot. As shown in Figure 4A, nm23-H1 siRNA significantly decreased nm23-H1 expression in 6-10B cells, whereas its expression was not significantly suppressed by control siRNA. The effects of nm23-H1 knockdown by siRNA on the 6-10B cell invasion using an in vitro invasion assay was evaluated. As shown in Figures 4B and 4C, invasive 6-10B cells by transfection with the nm23-H1 siRNA were about 2.1-fold more than those by transfection with control siRNA

($P < 0.01$), indicating that knockdown of nm23-H1 in 6-10B cells increased in vitro invasive ability, and nm23-H1 expression levels were negatively associated with the invasive capacity of 6-10B cells.

2.5 nm23-H1 expression in primary and metastatic NPC

Immunohistochemistry was performed to detect the expression of nm23-H1 protein in the 93 primary NPC tissues and 20 cervical LMNPC tissues. As shown in Figure 5 and Table 2, nm23-H1 was significantly downregulated in LMNPC vs primary NPC ($P < 0.01$), indicating that the expression level of nm23-H1 was negatively associated with NPC metastasis.

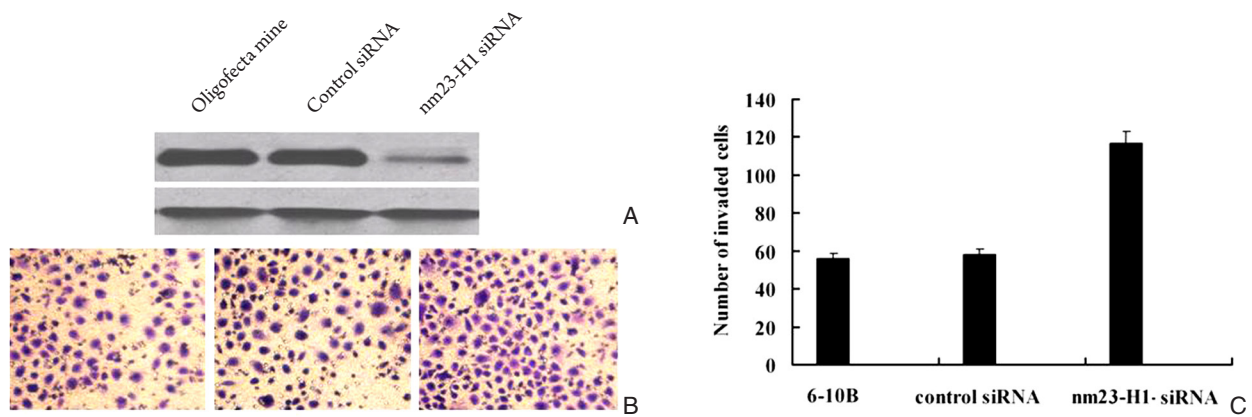


Figure 4 In vitro cell invasion assay of the nm23-H1 siRNA-transfected and control 6-10B cells. A: Western blot showing the expression levels of nm23-H1 in nm23-H1 siRNA-transfected and control 6-10B cells; B: Invasion of nm23-H1 siRNA-transfected and control 6-10B cells was measured by using transwell chambers. Tumor cells penetrating the pre-coated polycarbonate membrane were photographed ($\times 100$). C: Average numbers of invasive tumor cells per field in nm23-H1 siRNA-transfected and control 6-10B cells.

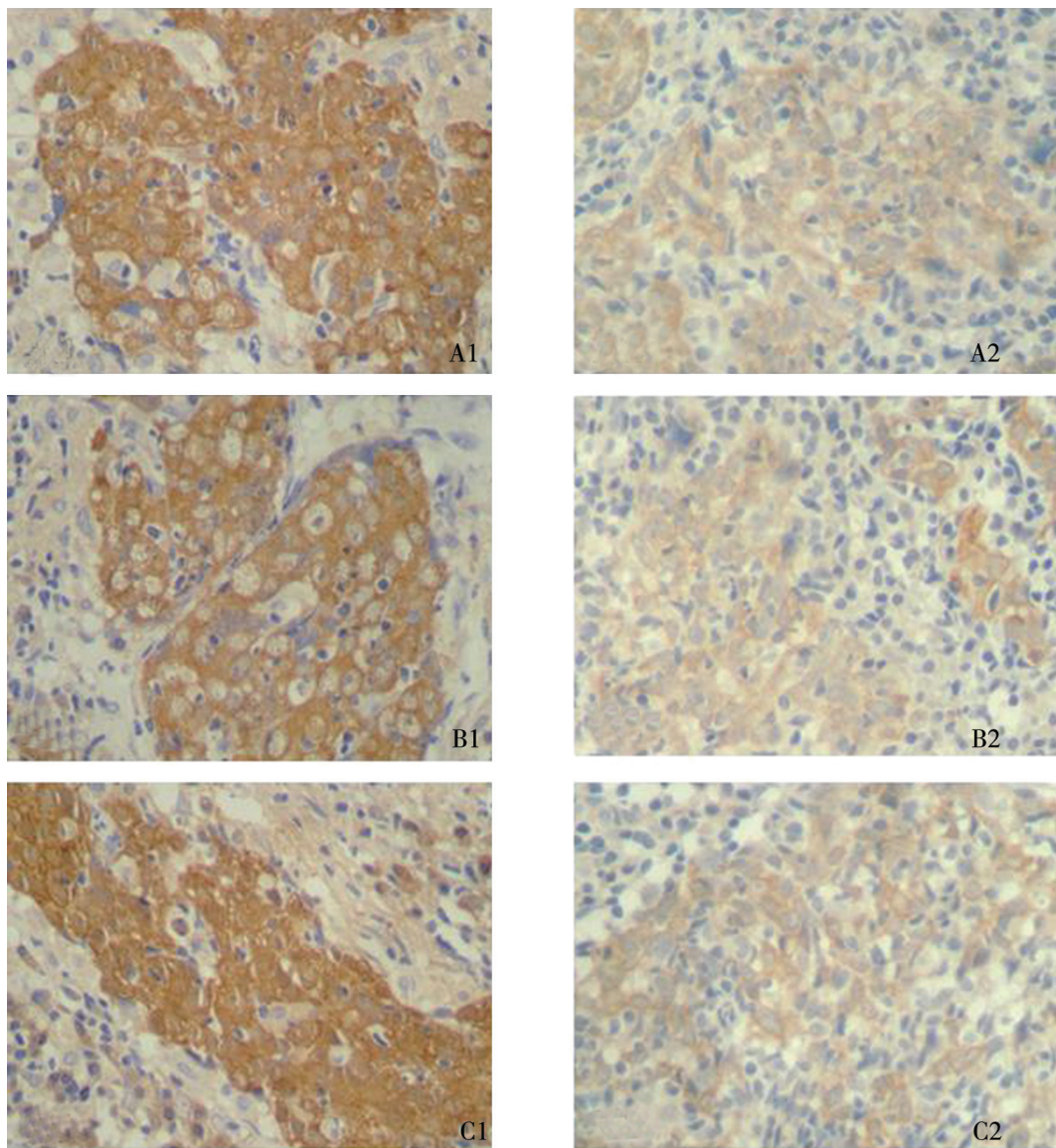


Figure 5 Representative results of immunohistochemistry of nm23-H1 in the primary NPC (A1, B1, C1) and LMNPC (A2, B2, C2). (Original magnification, $\times 200$).

Table 2 Difference of nm23-H1 expression in primary NPC and LMNPC

Tissues	Expressional levels(Staining score)			Total	P
	Negative(0~2)	Moderate(3~4)	Strong(5~6)		
NPC	15	37	41	93	0.001
LMNPC	11	6	3	20	

2.6 Correlation of nm23-H1 expression in primary NPC with clinicopathologic factors and clinical outcomes

Table 3 showed the correlation of several clinicopathological variables with nm23-H1 expression in 93 primary NPC tissues. Tumors with the lower level of nm23-H1 tended to have a more advanced clinical stage, more frequent recurrence, and regional lymphonode and distant metastasis ($P < 0.05$ or 0.01 , Table 3). These results indicated that the expression level of nm23-H1 in primary NPC was associated with the metastasis and disease progression.

Table 3 Relationships between nm23-H1 expression and clinicopathologic factors

	n	Expressional levels			P
		Negative	Moderate	Strong	
Gender/Male					
Male	62	28	25	9	0.645
Female	31	13	12	6	
Age					
≥50	28	12	11	5	0.813
<50	65	29	26	10	
Primary tumor (T) stage					
T ₁	11	5	4	2	0.938
T ₂	22	10	9	3	
T ₃	47	21	19	7	
T ₄	13	5	5	3	
Regional lymph node (N) metastasis					
N ₀	23	6	12	5	0.001
N ₁	44	18	18	8	
N ₂	15	9	5	1	
N ₃	11	8	2	1	
Distant metastasis(M)					
M ₀	85	34	36	15	0.033
M ₁	8	7	1	0	
Clinical stage					
II	33	9	17	7	0.025
III	50	23	19	8	
IV	10	9	1	0	
Recurrence					
Negative	65	20	32	13	0.002
Positive	28	21	5	2	

Survival curves were calculated for a total of 93 patients with NPC. At the end of the study, 43 patients (46.2%) had died of NPC, 2 patients (2.2%) had died of unrelated causes, 48 patients (51.6%) were still alive, 28 patients (30.1%) had a recurrence of the disease, and 8 patients (8.6%) showed distant metastasis. The follow-up period was 6 to 72 (48 ± 14.5) months. Using univariate analysis, the following variables were found significantly associated with prognosis: clinical stage, recurrence, regional lymphonode and distant metastasis, and the expression level of nm23-H1 ($P < 0.05$ or 0.01 ; Table 4). Survival curves showed that the survival rate of the patients with nm23-H1 up-regulation was significantly decreased ($P < 0.01$, Figure 6). Multivariate analysis showed that recurrence, regional lymphonode and distant metastasis, and expression level of nm23-H1 had an independent prognostic effect on overall survival ($P < 0.01$, Table 5).

Table 4 Prognostic factors by univariate analysis (Cox's proportional hazards model)

Variables	Hazard ratio(95% confidence interval)	P
Age (≥50/<50)	1.107(0.585-1.389)	0.637
Gender (male/female)	1.131(0.717-1.741)	0.625
TNM (II/III/IV)	1.447(0.522-1.958)	0.025
Recurrence (N/P)	2.343(1.318-3.287)	0.002
Distant metastasis (N/P)	1.627 (0.497-2.122)	0.005
Lymphonode metastasis (N/P)	1.527(0.897-2.152)	0.009
nm23-H1(0-2/3-4/5-6)	2.061(0.309-2.709)	0.000

N: Negative; P: Positive.

Table 5 Significant prognostic factors by multivariate analysis(Cox's proportional hazards model)

Variables	Hazard ratio (95% confidence interval)	P
TNM (II/III/IV)	0.817(0.476-1.113)	0.143
Recurrence (N/P)	4.131(0.996-6.206)	0.009
Distant metastasis (N/P)	3.104 (1.800-5.054)	0.000
Lymphonode metastasis (N/P)	2.903 (1.43-4.058)	0.008
nm23-H1(0-2/3-4/5-6)	2.614(0.336-3.871)	0.011

N: Negative; P: Positive.

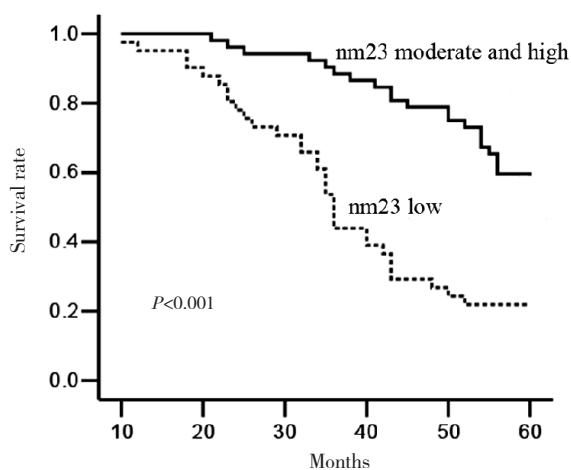


Figure 6 KaplanMeier survival curves according to expression levels of nm23H1 ($P=0.000$; A) in primary NPC.

3 Discussion

The five-year survival rate for NPC patients remains 50%-60% despite it is well responsive to radiotherapy, and the majority of patients surrender recurrence and metastasis after treatment^[5-6]. Therefore, identification of NPC metastasis-related proteins is important to commence the effective treatment and to improve survival for NPC patients, as well as may provide new insights into the metastatic mechanisms of NPC. Because the functional molecules in cells are proteins, proteome analysis is believed to have an advantage over cDNA microarray for clinical use. Differential proteome analysis of cancer cell lines with different metastatic potentials allows the identification of aberrantly expressed proteins associated with the metastasis^[9]. In this study, we compared the protein expression profiles of highly metastatic 5-8F and non-metastatic 6-10B NPC cell lines to identify the proteins related to NPC metastasis. A total of 15 differentially expressed proteins were identified by MS, and the differential expression levels of three identified proteins (nm23-H1, keratin 8, and annexin A1) in 5-8F and 6-10B cell lines were selectively confirmed by Western blot, suggesting that the proteins identified by comparative proteomic approach are actually differential expression proteins in the two cell lines.

nm23-H1 downregulated in 5-F cells is one of the proteins known to play a role in tumor metastasis. Its role in tumor metastasis was initially identified based on its reduced expression in murine melanoma cells with high metastasis potentials^[16]. Subsequent studies have revealed that the expression level of nm23-H1 is negatively correlated with the metastatic potential of certain human tumors such as melanoma and breast

carcinoma^[17], indicating a metastasis-suppressing role of nm23-H1. Transfection and animal studies indeed support the idea that nm23-H1 acts as a metastasis suppressor in these types of tumors^[17]. However, these findings cannot be generalized, and the biological functions of nm23 in cancer cells are perplexed. A positive correlation between nm23-H1 level and metastatic potential has also been observed in other human tumors including neuroblastoma^[18], osteosarcoma^[19], pancreatic carcinoma^[20], and esophageal squamous cell carcinoma^[21]. Additionally, frequency of nm23 expression in clinical specimens varied among different cancers, and no consensual result of prognostic analysis was achieved. Some studies showed that nm23-H1 expression was indeed associated with a better prognosis^[22-25], while some studies revealed that nm23-H1 expression might in fact facilitate tumor development and disease progression, and overexpression of nm23-H1 is indicative of poor prognosis in the patients^[26-31]. The accumulating evidence indicated that nm23-H1 was involved in the metastasis of human malignant tumor, and its expression level was associated with the patient prognosis. However, the role of nm23 in NPC metastasis and its clinicopathological significance are also not properly defined. Thus, we further tested whether nm23-H1 inhibits NPC metastasis. Immunohistochemical results showed that nm23-H1 expression was obviously lower in LMNPC than in primary NPC, and the level of nm23-H1 expression in primary NPC was negatively associated with clinical metastasis, which indicated that nm23-H1 inhibited NPC metastasis. Furthermore, decreased nm23-H1 expression by siRNA significantly increased in vitro invasive ability of 6-10B NPC cell line. The results further supported that nm23-H1 behaves as a metastasis suppressor in human NPC.

In this study, the correlation of nm23-H1 expression in primary NPC with clinicopathological features and clinical outcomes were also evaluated. The results showed that nm23-H1 downregulation in primary NPC was significantly correlated with lymph node and distant metastasis, advanced clinical stage and recurrence. Survival curves showed that the NPC patients with nm23-H1 downregulation in primary NPC had a poor prognosis. Multivariate analysis confirmed that nm23-H1 expression level was an independent prognostic indicator. These data indicate that nm23-H1 downregulation in NPC is associated with a poor prognosis and disease progression. In summary, we identified 15 proteins possibly associated with NPC metastasis by proteomic approach. We further showed that nm23-H1 downregulation is associated with NPC metastasis, and downregulation of nm23-H1 in the NPC is a biomarker for poor prognosis.

References

1. Yu MC, Yuan JM. Epidemiology of nasopharyngeal carcinoma[J]. *Semin Cancer Biol*, 2002(6), 12:421-429.
2. Ho JHC. An epidemiologic and clinical study of nasopharyngeal carcinoma[J]. *Int J Radiat Oncol Biol Phys*, 1978, 4(3/4):183-198.
3. King AD, Ahuja AT, Leung SF, et al. Neck node metastases from nasopharyngeal carcinoma: MR imaging of patterns of disease [J]. *Head Neck*, 2000, 22(3): 275-281.
4. Huang CJ, Leung SW, Lian SL, et al. Patterns of distant metastases in nasopharyngeal carcinoma[J]. *Kaohsiung J Med Sci*, 1996, 12(4):229-234.
5. Lee AW, Poon YF, Foo W, et al. Retrospective analysis of 5037 patients with nasopharyngeal carcinoma treated during 1976-1985: overall survival and patterns of failure[J]. *Int J Radiat Oncol Biol Phys*, 1992, 23(2): 261-270.
6. Leung SF, Teo PM, Shiu WW, et al. Clinical features and management of distant metastases of nasopharyngeal carcinoma[J]. *J Otolaryngol*, 1991, 20(1):27-29.
7. Lung HL, Bangarusamy DK, Xie D, et al. THY1 is a candidate tumour suppressor gene with decreased expression in metastatic nasopharyngeal carcinoma[J]. *Oncogene*, 2005, 24(43): 6525-6532.
8. Fang WY, Liu TF, Xie WB, et al. Reexploring the possible roles of some genes associated with nasopharyngeal carcinoma using microarray-based detection[J]. *Acta Biochim Biophys Sin (Shanghai)*, 2005, 37(8):541-546.
9. Reymond MA, Schlegel W. Proteomics in cancer[J]. *Adv Clin Chem*, 2007, 44: 103-142.
10. Song LB, Yan J, Jian SW, et al. Molecular mechanisms of tumorigenesis and metastasis in nasopharyngeal carcinoma cell sublines[J]. *Ai Zheng*, 2002, 21(2): 158-162.
11. Wu YT, Wang HM, Yang XP. Establishment and characterization of a xenografted nasopharyngeal carcinoma and corresponding epithelial cell line[J]. *Ai Zheng*, 1995, 14(3):83-88.
12. Song LB, Wang HM, Zheng M. Study on the tumor heterogeneity of nasopharyngeal carcinoma cell line (SUNE-1)[J]. *Ai Zheng*, 1998, 17(2): 324-327.
13. Qian CN, Guo X, Cao B, et al. Met protein expression level correlates with survival in patients with late-stage nasopharyngeal carcinoma[J]. *Cancer Res*, 2002, 62(2):589-596.
14. Yang YX, Xiao ZQ, Chen ZC, et al. Proteome analysis of multidrug resistance in vincristine-resistant human gastric cancer cell line SGC7901/VCR[J]. *Proteomics* 2006, 6(6):2009-2021.
15. Cheng AL, Huang WG, Chen ZC, et al. Identification of novel biomarkers for differentiation and prognosis of nasopharyngeal carcinoma by laser capture microdissection and proteomic analysis[J]. *Clin Cancer Res*, 2008, 14(2):435-445.
16. Steeg PS, Bevilacqua G, Kopper L, et al. Evidence for a novel gene associated with low tumor metastatic potential[J]. *J Natl Cancer Inst*, 1988, 80(3):200-204.
17. Hartsough MT, Steeg PS. nm23/nucleoside diphosphate kinase in human cancers[J]. *J Bioenerg Biomembr*, 2000, 32(3):301-308.
18. Almgren MA, Henriksson KC, Fujimoto J, et al. Nucleoside diphosphate kinase A/nm23-H1 promotes metastasis of NB69-derived human neuroblastoma [J]. *Mol Cancer Res*, 2004, 2(7): 387-394
19. Oda Y, Naka T, Takeshita M, et al. Comparison of histological changes and changes in nm23 and c-MET expression between primary and metastatic sites in osteosarcoma: a clinicopathologic and immunohistochemical study[J]. *Hum Pathol*, 2000, 31(6): 709-716.
20. Nakamori S, Ishikawa O, Ohhigashi H, et al. Expression of nucleoside diphosphate kinase/nm23 gene product in human pancreatic cancer: an association with lymph node metastasis and tumor invasion[J]. *Clin Exp Metastasis*, 1993, 11(2): 151-158.
21. Wang LS, Chow KC, Lien YC, et al. Prognostic significance of nm23-H1 expression in esophageal squamous cell carcinoma[J]. *Eur J Cardiothorac Surg*, 2004, 26(2):419-424.
22. Hennessy C, Henry JA, May FE, et al. Expression of the antimetastatic gene nm23 in human breast cancer: an association with good prognosis[J]. *J Natl Cancer Inst*, 1991, 83(4): 281-285.
23. Florenes VA, Aamdal S, Myklebost O, et al. Levels of nm23 messenger RNA in metastatic malignant melanomas: inverse correlation to disease progression[J]. *Cancer Res*, 1992, 52(21): 6088-6091.
24. Nakayama T, Ohtsuru A, Nakao K, et al. Expression in human hepatocellular carcinoma of nucleoside diphosphate kinase, a homologue of the nm23 gene product[J]. *J Natl Cancer Inst*, 1992, 84(17):1349-1354.
25. Hsu NY, Chow KC, Chen WJ, et al. Expression of nm23 in the primary tumor and the metastatic regional lymph nodes of patients with gastric cardiac cancer[J]. *Clin Cancer Res*, 1999, 5(7): 1752-1757.
26. Haut M, Steeg PS, Willson JK, et al. Induction of nm23 gene expression in human colonic neoplasms and equal expression in colon tumors of high and low metastatic potential[J]. *J Natl Cancer Inst*, 1991, 83(10): 712-716.
27. Zou M, Shi Y, al-Sedairy S. High levels of nm23 gene expression in advanced stage of thyroid carcinomas[J]. *Br J Cancer*, 1993, 68(2): 385-388.
28. Müller W, Schneiders A, Hommel G, et al. Expression of nm23 in gastric carcinoma: association with tumor progression and poor prognosis[J]. *Cancer*, 1998, 83(12):2481-2487.
29. Pavelić K, Kapitanović S, Radošević S, et al. Increased activity of nm23-H1 gene in squamous cell carcinoma of the head and neck is associated with advanced disease and poor prognosis[J]. *J Mol Med*, 2000, 78(2): 111-118.
30. Niitsu N, Nakamine H, Okamoto M, et al. Expression of nm23-H1 is associated with poor prognosis in peripheral T-cell lymphoma[J]. *Br J Haematol*, 2003, 123(4): 621-630.
31. Bosnar MH, Pavelić K, Krizanac S, et al. Squamous cell lung carcinomas: the role of nm23-H1 gene[J]. *J Mol Med*, 1997, 75(8): 609-613.

(Edited by PENG Minning)